

Advanced Materials Research

Eduardo Alves

The Advanced Materials Research Group (GIMA) operates most of the experimental facilities at the Ion Beam Laboratory (IBL). The IBL is equipped with a 2.5 MV Van de Graaff accelerator with a nuclear microprobe and external beam facility; a 3 MV tandem accelerator with a 30 μm lateral resolution Accelerator Mass Spectrometry (AMS) system; a high flux Danfysik S1090 ion implanter.

The group explores and develops ion beam techniques to study advanced materials with high technological impact, e.g. wide band gap semi-conductor nanostructures, oxides and functional materials in collaboration with a long list of other groups. Among the wide band gap materials our major interests are focused on III-nitrides and ZnO. These alloys are the base of an emerging class of optoelectronic devices operating in the visible wavelength range of the electromagnetic spectrum being under intense research worldwide. Our work aims at the optimization of the implantation conditions of magnetic and optically active dopants in these materials. In addition an intense research on the structural properties and Rare Earth doping of GaN/AlN QD layers continued in collaboration with Universities of Aveiro, Grenoble and Strathclyde.

The work in oxides aims at modification of the optical and structural properties of $\alpha\text{-Al}_2\text{O}_3$ as well as the study of magnetic doping of ZnO by ion implantation. The potential of these materials for spintronics applications is being investigated with University of Aveiro and the University of Lisboa.

Taking advantage of the versatility of ion beam techniques to study thin films and multilayers, important work continued on the characterisation of magnetic thin films for magnetic spin valves, tunnel junctions, and functional oxynitride coatings, in

collaboration with INESC, University of Minho and New University of Lisbon.

The activities under the technology programme of the European Fusion Development Agreement (EFDA), in association with Instituto de Plasmas e Fusão Nuclear (IPFN) was focused on the study of beryllium intermetallics and the study of surface erosion and redeposition processes as well as ^2H retention in JET tiles.

Training and Education continued as a major commitment of the group through the supervision of M.Sc. and Ph.D. thesis.

All the referred activities are funded by projects, either European or National (FCT), in collaboration with other Institutions. Of particular importance are the projects funded by the EC, “*FEMaS-Fusion Energy Material Science*”, EURATOM 7th Framework Programme for Nuclear Research and Training, Grant agreement No 224752-CA, (2008-2011) and “*Support of Public and Industrial Research Using Ion Beam Technology (SPIRIT)*”, Grant agreement No 227012-CP-CSA-Intra (starting date 2009/03/01) and EFDA JET Technology Workprogramme JW11-FT-3.59. The external collaborations allowed a continuous exchange of expertise and mobility of researchers, a key condition to keep the scientific activity of the group at the forefront of research and its international recognition in the field of processing and characterization of advanced materials with ion beams.

Publications (peer reviewed journals): 45

Proceedings Books: 12

Conference and workshop contributions: 3 invited, 19 oral and 27 posters.

Running projects: 18

Researchers^(*)

E. ALVES, Princ. (Group Leader) (85%)

R.C. SILVA, Princ.

L.C. ALVES, Aux. (75%)

U. WAHL, Princ. (25%)

K. LORENZ, (FCT) (85%)

V. DARAKCHIEVA, (FCT)

V. CORREGIDOR, (FCT)

A.R. RAMOS, Aux. (10%)

A. KLING, Aux. (10%)

N.P. BARRADAS, Princ. (15%)

A.C.MARQUES, Post-Doc. (FCT)

M. DIAS, Post-Doc.

N.B.SEDRINE, Post-Doc.

N.FRANCO, Post-Doc, (FCT)

P. JANA, Post-Doc, (SPIRIT)

R. MARTINS, Post-Doc, (FCT)

A.REDONDO-CUBERO, Post-Doc, (FCT)

Students

B. M. NUNES, Ph.D. (FCT)

C. BOUHAFS, Project Grant (FCT)

I. FIALHO, Ph.D. Project Grant (SPIRIT)

L.M. PEREIRA, Ph.D. (FCT)

M.A. MERCIER, Student (IST)

N. CATARINO, Project Grant (SPIRIT)

S. MAGALHÃES, Ph.D. (FCT)

S. MIRANDA, Project Grant (FCT)

Collaborators

A. RODRIGUES

C.P. MARQUES

J.V. PINTO

J.G. LOPES

M.VILARIGUES

R. MATEUS

Technical Personnel

J. ROCHA

F. BAPTISTA

P. PEREIRA

() Also members of CFNUL.*



Connecting the external proton beam at ITN with silver art objects

V. Corregidor, L.C. Alves, L. Penalva¹, B. Maduro¹,
A. J. Candeias², J. Mirão³

Objectives

The starting point of this work was the detection of kanji characters designed inside an oratory-reliquary, which belongs to the collection of the Museu Nacional de Arte Antiga (MNAA), Lisbon. This object, from the “Vidigueira Treasure”, was unquestionably assumed as the result of Indo-Portuguese work. Two other objects, with common origin, a pax “porta-paz” and a missal-bookshelf, are part of this “Vidigueira Treasure”.

One of the aims of the work is to perform an elemental compositional analysis of the pieces, using the non-destructive and sensitive capabilities of the micro-external beam setup installed at ITN, and then correlate the data with other coeval silver objects for establishing the provenance of the silver used to produce them.

Results

The first object to be analysed at ITN, was the pax. It was executed in silver partially golden and decorated with silver filigree. The results obtained by PIXE at several points show that an Ag:Cu alloy with Cu contents lower than 10 wt.% was used in the manufacture of the object. The higher Cu concentration (10 wt.%) was found in the interior filigree of the pediment. In all cases, the impurities detected were: Bi, Au, Pb, Hg, Zn, Fe and Ti. The presence and concentration of these impurities give information about the provenance, and so, similar values are expected to be found in the other objects from the Vidigueira Treasure, since the same origin is assumed. The results obtained will contribute to the establishment of a reference composition of the Indo-Portuguese Silver Jewellery. In the golden parts, some of them very deteriorated, only Au, Ag and Cu could be detected, confirming that the mercury gilding technique was not employed in this piece. The

analysis and combined information of the spectra simultaneously recorded using both IBA techniques, PIXE and RBS, allowed the determination of Au depth profile in the golden parts. Due to the state of conservation, the distribution of gold on the surface is non-homogeneous and a pure layer of Au could not be detected. Instead, a maximum concentration of Au at the surface, around 85 wt.%, was found in the back side. Gold diffusion lengths in the golden parts were always below 3 μm . The handle of the piece has a snake shape, performed in two parts joined by a gilded frieze. The PIXE elemental maps show the Au, Pb and Hg distribution along the joint (Fig. 1). The Pb and Hg may have been intentionally added during the welding process for reducing the melting point of the Ag:Cu alloy. The top of the main body of the oratory has a silver decorative element, with three small urns. Two of them were also analysed at ITN. Results show not only different Ag:Cu composition ratios for each one, 98:2 wt.% and 90:10 wt.%, but also the presence of different impurities such as Zn and Ni in the latter. Prior to this characterization the pieces were subjected to an exhaustive cleaning process of conservation and restoration and the patinas that were formed over the years have been removed.

Conclusion

It should be noticed that by using the IBA techniques it is also possible studying patinas formed on the surface of silver objects, mostly Ag_2S and AgCl . Although it is not possible to extract direct information on the chemical species formed, the possibility of obtaining 2D distribution of elements such as Cl and S allows inferring the formation of such compounds and define areas with different corrosion extent.

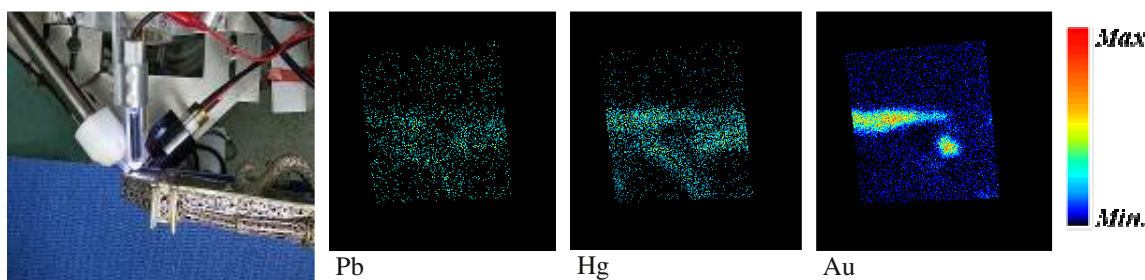


Fig. 1- Pax from the “Vidigueira Treasure” during the measurements at ITN. PIXE elemental maps of Pb, Hg and Au, $800 \times 800 \mu\text{m}^2$, from the joint of the handle with snake-shape.

¹ Museu Nacional de Arte Antiga. Rua das Janelas Verdes 1249 - 017 Lisboa, Portugal. ² IMC, Laboratório de Conservação e Restauro José de Figueiredo, Lisboa, Portugal. ³ Instituto HERCULES, Universidade de Évora, Portugal.

Defects identification on modern gold coins

V. Corregidor, L.C. Alves, J. Cruz

Commemorative coins, usually made of noble materials such as gold, minted by the Mint Offices of different countries, represent value added goods both for the Mint Officers and for the collectors.

In this sense, manufacture free of defects and good preservation conditions are of utmost importance. But sometimes, even under good preservation conditions coloured spots, often related with corrosion, appear on the surface of the coins. One of these coins, minted in 2006, revealing different types of defects in both faces, was analysed by PIXE at ITN. It was found that most of these defects are related with the presence of silver at the surface (Fig.1). The origin of silver can be related with contamination of the production line, where some silver particles may transfer to the surface of the gold strips. Afterwards, the different processes such as polishing procedures or contact with sulphur-containing contaminants, promote tarnishing of silver tarnish creating silver stains of different colours.

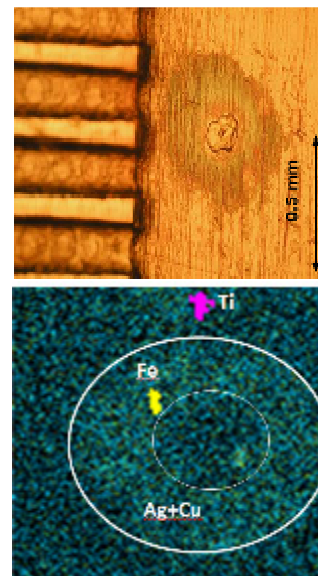


Fig.1 Stereomicroscopy photograph and PIXE compositional scan distribution of a Ag-rich defect with Fe and Ti.

Impurities evolution and patina formation on ancient Portuguese silver coins

V. Corregidor, L.C. Alves, N. Franco, J. Cruz

Ancient silver coins are usually a Ag:Cu alloy. The Cu was intentionally added in order to increase the hardness of the alloy. But other elements can be found in the composition resulting from the raw materials used to mint the coins. The presence of certain elements and its concentration can give information on the origin of the raw material and also on the period in which the coins were minted.

Portuguese silver coins from different centuries (XIX and XX) and provenance were analysed by PIXE. As a general tendency, the presence of impurities and their concentrations have decreased along time (Fig. 1): Ni, Au, Hg or Bi were not detected in the 1 rupia coins from 1912, but they are present in the coin of 6 *vinténs* of D. João VI (1816-1826). This tendency is not followed by the Pb concentration when we compare the same 6 *vinténs* of D. João VI (1816-1826) and 1/2 *rupia* from 1881.

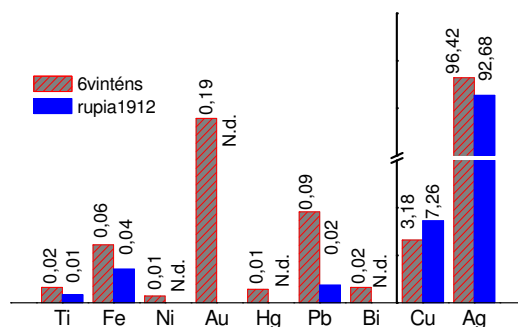


Fig. 1- Comparison of impurities concentration (at.%) found in two coins: 6 vinténs of D. João VI (1816-1826) and 1 rupia coin from 1912.

Characterization of historical tiles

S. Coentro,^{1,2} S. Muralha^{1,2}, M. Larsson¹, M. Vilarigues^{1,2}, V. Corregidor, L.C. Alves, R.C. da Silva

Historical tiles belonging to Convento de Sta Clara-a-Velha, Coimbra and to Palácio da Pena, Sintra, dated from the late Middle Ages to early Renaissance period but of uncertain provenance, have been characterized by nuclear microprobe analysis, as part of a collaboration project on early Portuguese tile production. Element identification allowed establishing the colour pigments used in the decoration of the tiles and the compositions of the glazes.



¹ DCR/FCT-UNL; ² VICARTE/FCT-UNL; ³ REQUINTE/FCT-UNL.

Determination of crystal ordering and lattice-site location in ZnO compounds: sublattice-resolved studies via ion channelling

A. Redondo-Cubero¹, R. Gago¹, A. Hierro², M. Vinnichenko³, J.-M. Chauveau⁴, G. Tabares², M. Krause³, A. Kolitch³, E. Muñoz², N. Franco, E. Alves, K. Lorenz

ZnO and MgZnO samples were studied by Rutherford Backscattering Spectrometry under channelling conditions (RBS/C). In ZnO samples, grown in c-plane orientation by pulsed magnetron sputtering, the defect formation was evaluated by RBS/C as a function of the substrate temperature. Interestingly, Zn-related defects are annealed at relatively low temperatures, while a high amount of O interstitials remain even for substrate temperatures up to 550 °C. These results point to a higher relevance of O-related defects for electronic properties and structure formation of undoped epitaxial ZnO films. In MgZnO samples, grown in a-plane orientation by molecular beam epitaxy, the lattice-site location of Mg was evaluated. Using the asymmetric shadowing effect for both Zn and O sites in RBS/C angular scans, the substitutional behaviour of Mg in Zn-sites was confirmed unambiguously for Mg contents as high as 56 %.

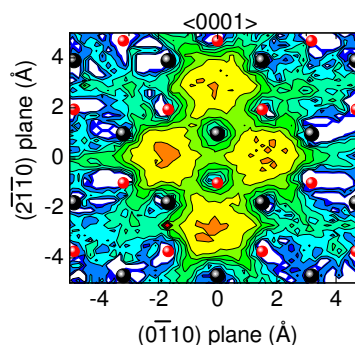


Fig. 1 Flux distribution of channelled particles in the c-axis of a wurtzite crystal (Redondo-Cubero et al., J. Appl. Phys. 110, 113516, 2011).

¹ Instituto de Ciencia de Materiales de Madrid, CSIC, Madrid, Spain.

² ISOM and DIE, ETSI Telecomunicación, Universidad Politécnica de Madrid, Madrid, Spain.

³ Institute of Ion Beam Physics and Materials Research, HZDR, Dresden, Germany.

⁴ Centre de Recherche sur l'HétéroÉpitaxie et ses Applications (CRHEA-CNRS), Valbonne Sophia Antipolis, France.

Cathodoluminescence of rare earth implanted Ga₂O₃ and GeO₂ nanostructures

E. Nogales¹, P. Hidalgo¹, K. Lorenz, B. Méndez¹, J. Piqueras¹, E. Alves

Rare earth (RE) doped gallium oxide and germanium oxide micro- and nanostructures, mostly nanowires, have been obtained and their morphological and optical properties characterized. Undoped oxide micro- and nanostructures were grown by a thermal evaporation method and were subsequently doped with gadolinium or europium ions by ion implantation. No significant changes in the morphologies of the nanostructures were observed after ion implantation and thermal annealing. The luminescence emission properties have been studied with cathodoluminescence (CL) in a scanning electron microscope (SEM). Both β -Ga₂O₃ and GeO₂ structures implanted with Eu show the characteristic red luminescence peak centred at around 610 nm. Sharpening of the luminescence peaks after thermal annealing is observed in Eu implanted β -Ga₂O₃, which is assigned to the lattice recovery. Gadolinium asimplanted samples do not show rare earth related luminescence. After annealing, optical activation of Gd³⁺ is obtained in both matrices and a sharp ultraviolet peak, centred at around 315 nm, is observed.

¹ Departamento de Física de Materiales, Universidad Complutense, 28040 Madrid, Spain

Low temperature implantation damage build-up in GaN with different surface orientations

K. Lorenz, A. Redondo-Cubero, N. Catarino, E. Alves, E. Wendler¹

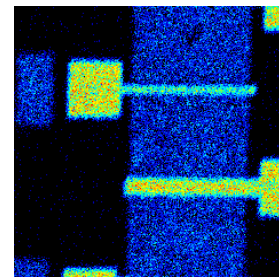
Detailed implantation studies have been performed in GaN epitaxial films grown along different crystal directions (c-plane, a-plane and m-plane material) using *in situ* Rutherford Backscattering Spectrometry /channelling at 15 K. Ar implantation at 15 K allows the study of damage build-up, minimizing thermal as well as chemical effects. Several stages could be distinguished in the damage formation processes. For low ion fluences an almost linear increase of damage with the ion fluence is observed attributed to the formation of point defects in isolated collision cascades (stage I). When the damaged regions produced by single ions start to overlap, vacancies and interstitials can recombine resulting in a plateau-like slow increase of the damage level (stage II). For higher fluences more stable defect complexes form (stage III) and the damage level increases steeply before reaching a second plateau (stage IV). For high fluences (stage V) GaN amorphizes. Up to stage III the damage curve is similar for all three crystal orientations. The saturation in stage IV however, takes place at a much lower level in a-plane material compared to c- and m-plane GaN. Enhanced dynamic annealing effects may be the reason for this pronounced difference or a certain type of defects that are shadowed by the atomic rows of the host material along certain directions.

¹ Institut für Festkörperphysik, Friedrich-Schiller-Universität Jena, Jena, Germany.

Study of ohmic contacts for GaN-based devices

A. Redondo-Cubero, L.C. Alves, M.F. Romero^{1,2}, M. Peroni³, C. Lanzieri³, A. Cetronio³, R. Gago⁴, M.D. Ynsa⁵, E. Alves, K. Lorenz, E. Muñoz¹

The in-depth diffusion and the lateral homogeneity of Au/Ni/Al/Ti ohmic contacts for AlGaIn/GaN high electron mobility transistors were analyzed by Rutherford Backscattering Spectrometry (RBS) and Particle Induced X-ray Emission (PIXE). Changing the thickness of the Al barrier layer, different surface morphologies were produced after the rapid thermal annealing. However, using the microprobe beam line at ITN, such morphologies could not be correlated with compositional variations within the resolution limits. Remarkably, RBS does show very large differences in the depth profiles of the metals with the increasing Al thickness. Such behaviour seems to be also linked to the production of ohmic contacts with low resistance.



PIXE map of transmission line models using the signal from the Au(M) line.

¹ ISOM and DIE, ETSI Telecomunicación, Universidad Politécnica de Madrid, Madrid, Spain.

² Institut für Experimentelle Physik, Otto-von-Guericke-Universität Magdeburg, Germany.

³ Selex Sistemi Integrati S.p.A. Via Tiburtina, Roma, Italy.

⁴ Instituto de Ciencia de Materiales de Madrid, CSIC, Madrid, Spain.

⁵ Centre of Micro-Analysis of Materials, Universidad Autónoma de Madrid, Madrid, Spain.

Composition, structure and morphology of Al_{1-x}In_xN thin films grown on Al_{1-y}Ga_yN templates with different GaN contents

S. Magalhães, K. Lorenz, N. Franco, E. Alves, S. Pereira¹, L. T. Tan², R.W. Martin², K.P. O'Donnell², I. M. Watson³

In this work we have studied the composition, structure and morphology of four Al_{1-x}In_xN thin films grown simultaneously on Al_{1-y}Ga_yN (y = 1, 0.93, 0.86, and 0.69) buffer layers by Metal Organic Chemical Vapour Deposition (MOCVD). A nominal InN content of ~16% was chosen to achieve closely lattice matched Al_{1-x}In_xN for the buffer layers with intermediate GaN molar fraction, a small tensile strain for growth on GaN, and compressive strain for the buffer layer with the lowest GaN fraction. Only the film deposited on GaN shows true pseudomorphic growth to the template. For growth on the ternary templates, the film roughness and the pit density increases with decreasing GaN content of the Al_{1-y}Ga_yN template due to the roughening of the growth templates themselves. While the macroscopic crystal quality of these ternary templates is quite homogeneous, the quality of the films varies significantly across the wafers. Results indicate that the structural and morphological quality of the templates does not only influence the structure and morphology of the films but also influence the strain state, the homogeneity and phase purity of the Al_{1-x}In_xN films.

¹ CICECO, Departamento de Física, Universidade de Aveiro, 3810-193 Aveiro, Portugal.

² Department of Physics, SUPA, University of Strathclyde, Glasgow, G4 0NG, U.K.

³ Institute of Photonics, SUPA, University of Strathclyde, Glasgow G4 0NW, U.K.

Study of CdTe nanorods grown on glass substrates

V. Corregidor, E. Alves, L.C. Alves, N. Sochinskii¹

Photovoltaic (PV) companies are actively involved in commercializing thin-film PV technologies using CdTe. In order to obtain higher efficiencies values, a new concept is under development. It is based in the use of nanostructured CdTe as the absorber layer. Nanorods of CdTe have already been successfully grown on sapphire substrates, but it is a critical issue the replication on commercial soda-lime glass. For this study, a monolayer of polyvinyl alcohol was deposited on the substrate prior to the deposition of bismuth, which acts as a catalyst material. The CdTe nanorods are grown by pulsed laser deposition using as a target a CdTe ingot previously grown by the Bridgman method. The samples were characterized by Rutherford Backscattering Spectrometry. The results indicate that the CdTe nanorods formation is very dependant on the processing parameters, specially the growth temperature. The composition of the CdTe nanorods is not stoichiometric: they all were found to be Te-rich, with concentration values up to 70 at%. Others catalyst materials such as NiCr or ZAO are under study.

¹ Consorzio C.R.E.O., Via Pile 60, I-67100 L'Aquila, Italy.

Effect of electron irradiation on the structural properties and photoluminescence of bulk HVPE GaN

M.-Y. Xie¹, A. Santos, E. Alves, T. Monteiro², N. T. Son¹, J. Rodrigues², A. Tolstoguzov³, A. Usui⁴, C. Hemmingson¹, B. Monemar¹, V. Darakchieva

Point defects have a strong effect on optical and electrical properties of materials, and their behaviour during device fabrication. We studied the effect of 2 MeV electron irradiation on the photoluminescence (PL) and structural properties of bulk GaN fabricated by HVPE.

Low-temperature PL reveals strong excitonic emission with well pronounced two-electron transitions and absence of DAP emission for the low electron concentration non-irradiated samples. Pronounced yellow luminescence (YL) is observed from the N-face GaN, while the Ga-face exhibits green luminescence (GL). PL measurements suggest that the GL is due to $V_{Ga}O^-$ while the YL is related to $V_{Ga}O^{2-}$. The electron irradiation results in an overall decrease of PL intensity indicating generation of non-radiative defects. In addition a UV band develops at ~ 3 eV upon electron irradiation. The irradiation leads to expansion of the lattice in both c and a directions, which could be associated with point defects in the Ga sublattice. Elemental analysis by SIMS and PL revealed inhomogeneous distribution of O along the GaN thickness, much higher in the N- side than in the Ga counterpart: different concentrations of the complexes formed by the irradiation induced point defects with O impurities may explain the changes observed in the lattice parameters of the N- and Ga-faces of bulk GaN.

¹ IFM, Linköping University, Sweden.

² Departamento de Física and i3N, Universidade de Aveiro, Portugal.

³ FCT, New University of Lisbon, Portugal.

⁴ R&D Division, Furukawa Co. Ltd., Japan..

Origin of n-type conductivity in InN grown by MOCVD

V. Darakchieva¹, M.Y. Xie¹, D. Rogalla², H.-W. Becker², K. Lorenz, E. Alves, N.P. Barradas, S. Ruffenach³, O. Briot³

The free electron concentrations, structural properties, and hydrogen depth profiles in as-grown and thermally annealed MOVPE InN films were studied. The quality of the MOVPE InN films – the dislocation and point defect densities, and electrical parameters – was found comparable to state-of-the-art MBE InN. Thermal annealing of the films resulted in lower free electron concentrations and increased electron mobilities. Enhanced H-concentrations were measured in the near-surface regions of the MOVPE InN films, similarly to MBE InN. Annealing lead to reduction in bulk H-concentration (Fig. 1) in correlation with decreasing the free-electron concentration, does not lead to any change in dislocation densities or strain in the films. The results suggest that hydrogen is a major source for unintentional n-type doping in MOVPE InN films.

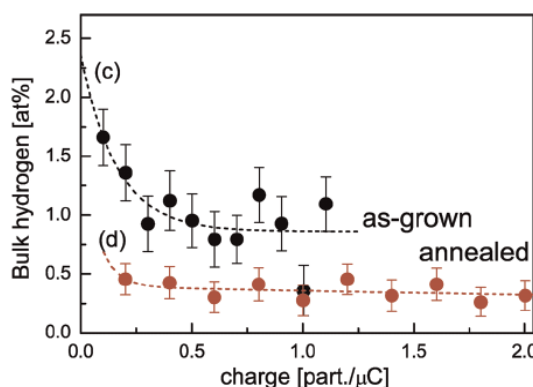


Fig. 1: Bulk hydrogen concentration versus the fluence for the as-grown (c) and annealed (d) MOVPE InN films.

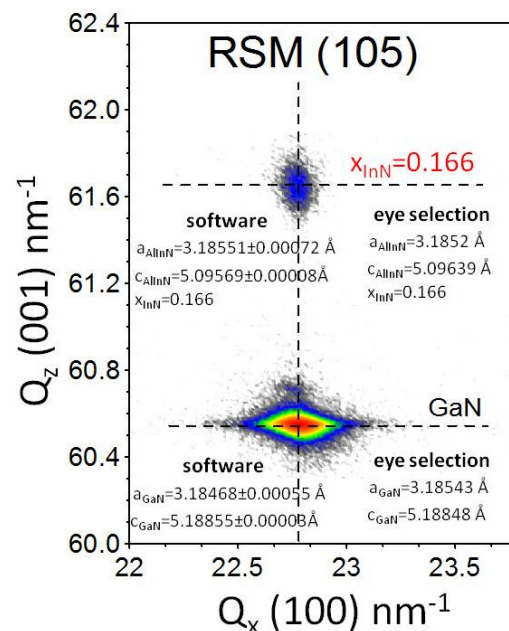
¹ Department of Physics, Chemistry, and Biology, Linköping University, 581 83 Linköping, Sweden.

² Ruhr-Universität Bochum, 44780 Bochum, Germany.

³ Groupe d'Etude des Semiconducteurs, Université Montpellier II, 34095 Montpellier, France.

High accuracy lattice parameter derivation from XRD reciprocal space maps
S. Magalhães, K. Lorenz, N. Franco, E. Alves

Lattice parameters of a crystal are fundamental physical quantities of any material and an accurate measurement of their absolute values is crucial. X-ray diffraction (XRD) reciprocal space maps (RSM) are often used to determine lattice parameters of thin heteroepitaxial films and allow the investigation of strains. The figure shows a RSM of a 100 nm thick $\text{Al}_{0.834}\text{In}_{0.166}\text{N}$ thin film grown pseudomorphically over a GaN buffer layer on a (0001) sapphire substrate. To analyse such a RSM, the lattice parameters of the GaN buffer were measured absolutely using the Bond method and the lattice parameters of the film were then determined relative to the GaN peak. For an automated analysis of such RSM, software was developed which extracts a large number of horizontal and vertical cuts through the RSM, performs peak fitting on these cuts and determines the maximum of each peak in the RSM. The main contribution to the uncertainties in the lattice parameters and compositions was found to be the error in the peak centres. The uncertainties are then estimated by adding in quadrature the uncertainties in the lattice parameters of the GaN buffer with the uncertainty the position of the $\text{Al}_{1-x}\text{In}_x\text{N}$ peak in the RSM. The resulting uncertainty in the InN molar fraction is below 0.1% absolute. The new program allows a more accurate determination of the lattice parameters and estimation of uncertainties.


Crystal quality enhancement of ternary AlGaIn alloys with high Al content by PA-MBE growth at low temperature
V. Fellmann¹, P. Jaffrennou¹, D. Sam-Giao¹, B. Gayral¹, E. Bellet-Amalric¹, B. Daudin¹, K. Lorenz, E. Alves

We have studied the influence of III/N flow ratio and growth temperature on the structural and optical properties of high Al-content (50–60%) AlGaIn layers grown by plasma-assisted molecular beam epitaxy. From Rutherford Backscattering Spectrometry we established that a flow ratio slightly above 1 produces layers with low amount of structural defects. Under this optimal III/N flow ratio, we found that optimal temperatures for growth of $\text{Al}_{0.5}\text{Ga}_{0.5}\text{N}$ layers with compositional homogeneity correlated with narrow UV photoluminescence are in the low temperature range for growing GaN layers, i.e. 650–680 °C. We propose that lowering the Ga adatom diffusion on the surface favours random incorporation of both Ga and Al adatoms in wurtzite crystallographic sites leading to the formation of a homogeneous alloy.

¹ CEA Grenoble, Département de Recherche Fondamentale sur la Matière Condensée/SP2M, Grenoble 38054, France.

Ion implantation of Cd in AlN
S.M.C. Miranda, N. Franco, E. Alves, K. Lorenz

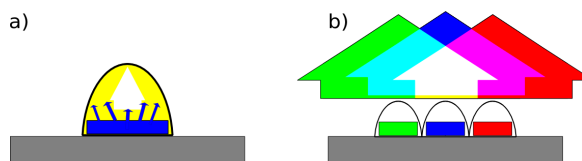
AlN based semiconductor performance is hampered by the lack of an efficient p-type dopant. In order to shed more light on this topic AlN thin films were implanted with cadmium (a possible alternative to Mg for p-type doping), to fluences of 1×10^{13} at/cm² and 8×10^{14} at/cm². The implanted samples were annealed at 950 °C under flowing nitrogen. The implantation damage could be fully removed for the lower fluence, while for the higher fluence the crystal quality was only partially recovered. For the high fluence sample the lattice site location of the ions was studied by Rutherford Backscattering/channelling (RBS/C): Cd ions were found to be incorporated in substitutional Al sites and no diffusion is seen upon thermal annealing. The observed high solubility limit and site stability are prerequisite for using Cd as p-type dopant in AlN.

Solid State Lighting Redefined by Bandgap Engineering Techniques

K. Lorenz, M. Auf der Maur¹, A. Di Carlo¹, K.P. O'Donnell²

The design strategy presently employed to obtain 'white' light from semiconductors combines the emission of an InGaN blue or UV light-emitting diode (LED) with that of one or more yellow-orange phosphors. While commercially successful, this approach suffers from energy losses during the absorption and reemission processes; compared to the alternative of combining 'true' red, green and blue (RGB) sources, it is intrinsically inefficient.

The two major roadblocks to the RGB approach are 1) the green gap in the internal quantum efficiency (IQE) of LEDs and 2) the diode droop in the efficiency of LEDs at higher current densities. The physical origin of these effects, in the case of III-nitrides, is generally thought to be a combination of Quantum Confined Stark Effect (QCSE) and Auger Effect (AE). These effects respectively reduce the electron-hole wavefunction overlap of In-rich InGaN quantum wells (QW), and provide a non-radiative shunt for electron-hole recombination, particularly at higher excitation densities. We developed a novel band gap engineering strategy based upon graded QWs that offers solutions to both of the roadblocks mentioned above. Its potential is tested by the results of simulations of green InGaN diodes performed using TiberCAD device modelling suite, which calculates the macroscopic properties of real-world optoelectronic and electronic devices in a multiscale formalism.



Schematics of the two main approaches to achieve white light using LEDs: a) A blue or UV LED is combined with a yellow (or multi-colour) emitting phosphor. b) Combination of three LEDs emitting in the green, blue and red.

¹ Department of Electronic Engineering, University of Rome "Tor Vergata", Italy;

² SUPA Department of Physics, University of Strathclyde, Glasgow G4 0NG, Scotland UK.

Experimental determination of the bandgap of epitaxial rhombohedral BN

N. Ben Sedrine, M.-Y. Xie,¹ N. Franco, M. Chubarov,¹ A. Henry¹, V. Darakchieva¹

Boron nitride (BN) has unique physical and chemical properties, such as strong planar covalent bonds but weak interactions between its basal planes, high thermal and chemical stabilities. In order to develop BN as a UV optoelectronic material, it is important to reliably determine the optical band-gap energy, E_g . All BN forms have a wide bandgap; however, despite extensive experimental and theoretical studies for cubic BN, wurtzite BN and hexagonal (h)-BN, little is known about rhombohedral (r)-BN. We have performed spectroscopic ellipsometry and cathodoluminescence spectroscopy of r-BN films grown by chemical vapour deposition on sapphire substrate. The ellipsometric data modelling of the 400nm-thick BN layer using Cauchy model, reveals the uniaxial nature of the r-BN film with ordinary and extraordinary dielectric responses for direction of light polarization parallel and perpendicular to the sample surface, respectively. We have determined the band-gap energies of r-BN $E_{g,ord} = 5.314$ eV (233 nm) and $E_{g,extraord} = 5.671$ eV (218 nm) from the calculated absorption coefficient α for the respective polarizations. Our results indicate that the band gap of r-BN is very close to the values reported previously for h-BN. Additional structural analysis further indicates that previous works might have erroneously assigned the band gap of r-BN to h-BN and calls for new experimental and theoretical works.

¹ IFM, Linköping University, SE-581 83 Linköping, Sweden.

Ageing effects on the wettability behaviour of laser textured silicon

B. Nunes, A. P. Serro^{2,3}, V. Oliveira^{4,5}, M. F. Montemor⁵, E. Alves, B. Saramago², R. Colaço¹

We investigate the ageing of acid cleaned femtosecond laser textured <100> Si surfaces. Changes in the surface structure and chemistry were analysed by Rutherford Backscattering Spectrometry (RBS) and X-ray photoelectron spectroscopy (XPS), in order to explain the time evolution of the water contact angles with the laser textured surfaces. It is shown that highly hydrophobic Si surfaces are obtained immediately after laser texturing and cleaning with acid solutions (water contact angle > 120°). However these surfaces are not stable and ageing leads to a decrease of the water contact angle which reaches a value of 80°. XPS analysis of the surfaces shows that the growth of the native oxide layer is most probably responsible for this behaviour.

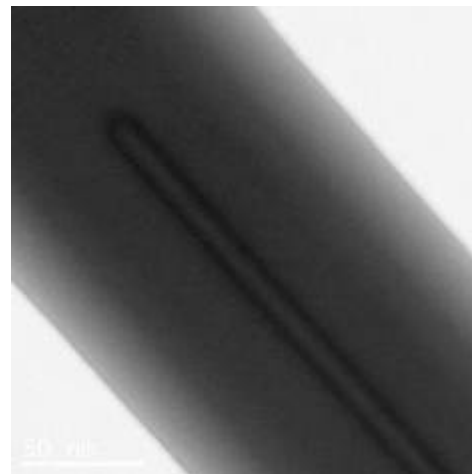
¹Departamento de Engenharia de Materiais, IST, PT; ²Centro de Química Estrutural, IST, Portugal; ³Instituto Superior de Ciências da Saúde Egas Moniz, PT; ⁴ISEL, PT; ⁵ICEMS, IST, Portugal.

Optical properties of InAsP/InP core shell nanowires grown by molecular beam epitaxy

C. Bouhafs, N. Ben Sedrine, L. Samet¹, D. Lindgren¹, B. Monemar¹, J. C. Harmand¹, R. Chtourou¹, V. Darakchieva

We have studied InAsP/InP core shell nanowires grown using molecular beam epitaxy (MBE) on InP (111) B substrate. The structural properties have been investigated using transmission electron microscopy (TEM) and scanning electron microscopy (SEM). The crystal structure of the InAsP core is wurtzite without defects and the crystal structure of the InP shell is mainly wurtzite with thin slices of zincblende inserted randomly on the top of the wire as seen in the figure. The diameter of the InAsP is around 20 nm (below Bohr radius of the InAsP) allowing the 2D confinement in the nanowires.

The optical properties have been investigated using micro-photoluminescence (μ PL) and photoluminescence as function of temperature (from 7.8 to 180 K) and excitation power density, which confirmed the confined nature of the bound excitons.



¹ IFM, Linköping University, SE-581 83 Linköping, Sweden.

Enhanced dynamic annealing and optical activation of Eu implanted a-plane GaN

N. Catarino, E. Nogales¹, N. Franco, V. Darakchieva, S.M.C. Miranda, B. Méndez¹, E. Alves, J.G. Marques, K. Lorenz

The implantation damage build-up and optical activation of a- and c- GaN epitaxial films was studied upon 300 keV Eu implantation at room temperature. The implantation defects cause an expansion of the lattice normal to the surface, i.e. along the a-direction in a-GaN and along the c-direction in c-GaN. The defect profile is bimodal with a pronounced surface damage peak and a second damage peak deeper in the bulk in both cases. For both surface orientations, the bulk damage saturates for high fluences. Interestingly, the saturation level for a- GaN is nearly three times lower than that for c-plane material suggesting very efficient dynamic annealing and strong resistance to radiation. a-GaN also shows superior damage recovery during post-implant annealing compared to c-GaN. For the lowest fluence, damage in a-GaN was fully removed and strong Eu related red luminescence is observed. Although some residual damage remained after annealing for higher fluences as well as in all c-plane samples, optical activation was achieved in all samples revealing the red emission lines due to the $^5D_0 \rightarrow ^7F_2$ transition in the Eu^{3+} ion. The present results demonstrate great promise for the use of ion beam processing for a-GaN based electronic devices as well as for the development of radiation tolerant electronics.

¹ Departamento de Física de Materiales, Universidad Complutense, 28040 Madrid, Spain.

Damage formation and recovery in Fe implanted 6H-SiC

P. Miranda, U. Wahl, N. Catarino, K. Lorenz, J.G. Correia, E. Alves

In order to study the damage formation and Fe lattice site location we have implanted 6H-SiC single crystals with $^{56}\text{Fe}^+$ ions with an energy of 150 keV, at fluences of $5 \times 10^{14} \text{ Fe}^+/\text{cm}^2$ and $1 \times 10^{16} \text{ Fe}^+/\text{cm}^2$ at different temperatures. The samples were subsequently annealed up to 1500 °C in vacuum in order to remove the implantation damage. The results show that the amorphisation is avoided by implanting at temperatures above 250 °C. For the samples implanted at lower temperatures, the amorphous layer regrows epitaxially at 1500 °C. The recrystallization induces the redistribution of the Fe ions in the implanted region with some segregation towards the surface, but the total amount of Fe is conserved. The samples implanted above the critical temperature that avoids amorphisation reveal a high fraction of Fe incorporated into regular sites along the [0001] axis. After the annealing at 1000 °C, a maximum fraction of ~75%, corresponding to a total of $3.8 \times 10^{14} \text{ Fe}^+/\text{cm}^2$, was measured in regular sites along the [0001] axis.

Position-sensitive detectors for use in RBS/Channelling studies

P. Miranda, U. Wahl, J.G. Correia, E. Alves, E. Bosne¹, M.R. Silva², M. Campbell³, L. Tlustos³, X. Ll. Cudie³

We have investigated the possibilities for the use of 2-dimensional position-sensitive detectors (PSDs) in RBS/C studies. For that purpose two types of PSDs were tested with 2 MeV ⁴He particles: a) a 1x1 cm² Si diode working with resistive charge division (RCD), b) a 256x256 pixel 1.5x1.5 cm² TimePix detector. Both detector types were able to process count rates of ~1 kHz, however, the energy resolution of the RCD PSD (34 keV FWHM) was somewhat superior to the TimePix (55 keV). While a position resolution of 160 μm (standard deviation) was achieved with the RCD PSD, the position resolution of TimePix is superior due to its 55 μm pixel size. However, in both cases the angular resolution of the measurement is dominated by the size of the ⁴He beam spot, collimated to 0.5 mm. For typical experimental geometries, angular resolutions around σ = 0.12° (RCD PSD) and σ = 0.06° (TimePix) are achieved. The most promising fields of application for both types of detectors are considered to be strain measurements in thin films and lattice location studies of heavy impurities.

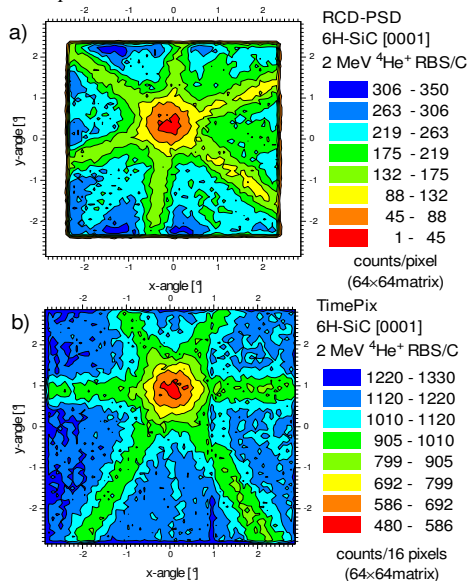


Fig. 1- Blocking patterns of 2 MeV ⁴He⁺ backscattered around the [0001] axis of a 6H-SiC crystal, measured with the a) RCD PSD, b) TimePix detector.

¹Departamento de Física and CICECO, Universidade de Aveiro, Portugal.

²Instituto Superior Técnico and Centro de Física Nuclear da Universidade de Lisboa, Portugal.

³MEDIPIX, CERN, 1211 Geneva 23, Switzerland.

Laser grooved buried contacts (LGBC) on silicon solar cells for low concentration purposes

V. Corregidor, L.C. Alves, J. Wemans¹, G. Sorasio¹

At a certain solar concentration level the efficiency of solar cells decreases due to power dissipation. One of the main factors responsible for this behaviour is the front metal grid, which should be optimized as well as the grid shading factor. For silicon solar cells working at low concentration levels (up to 10 times), the LGB contacts are an attractive solution for the production of low-cost concentrator cells able to handle the large current densities produced under concentration conditions. Silicon cells with LGB contacts, manufactured by NaREC and bought by the WS Energia, were characterized by PIXE. When the edge of a cell is analysed the Cu-rich buried contact can be clearly observed (Fig. 1). It is shown as well that the copper metallization also contains some Ni. On the other hand, Ag is only in the front surface with an irregular pattern. It is crucial to obtain a homogeneous distribution of the elements along the contacts since even under low concentration conditions, ohmic losses at the grid metal-semiconductor interface are critical to the efficiency of the cell.

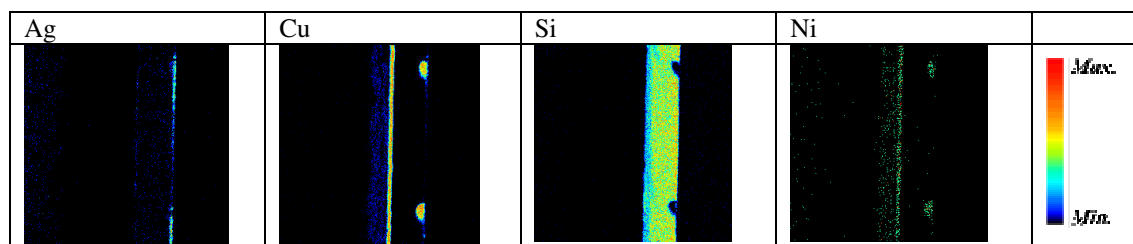


Fig. 1- 530x530 μm² PIXE maps. Elemental distribution of Ag, Si, Cu and Ni in the edge of the cell. Two fingers of the front metallization grid are shown.

¹ WS Energia SA, Taguspark Edifício Tecnologia II, Pav.46, 2740-257, Porto Salvo, Portugal.

Generation of defects on CdZnTe (CZT) detectors due to metallisation

V. Corregidor, E. Alves, Q. Zheng¹, F. Dierre¹, J. Crocco¹, H. Bensalah¹, E. Diéguez¹

The influence of deposition methods and type of metal (Au, Pt and Ru) contacts on the defects generated at the metal/semiconductor interface has been investigated by means of photoluminescence (PL) at low temperature, current-voltage characteristics, RBS and gamma response. Among the metals studied, Au and Pt have the best I-V characteristic curves and gamma response. In all cases there is a tellurium oxide layer between the substrate and the contact, but in the case of the thermal evaporation method this layer is very thin. In the case of the electroless method there is a wide (750×10^{15} at/cm²) interface with a strong mixing of Au, TeO₂ and CZT. This inter-diffusion mechanism is clearly observed in the A-center region of the PL spectra and in the increase of the (A-X) intensity line. The gold contacts deposited by electroless method showed the best results in terms of gamma response and I-V ohmic behaviour.

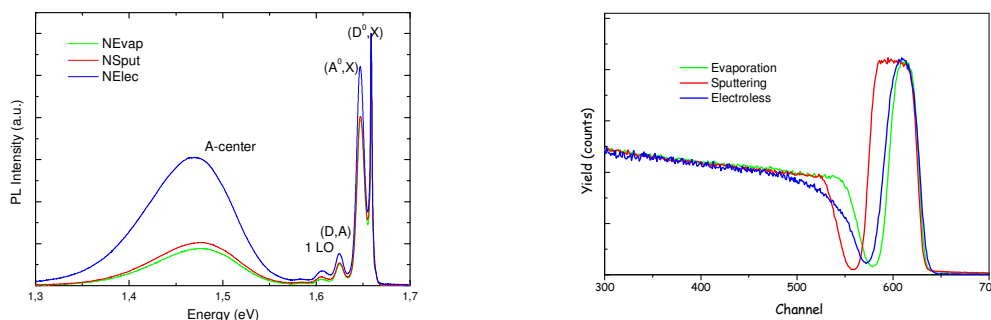


Fig. 1- The PL and the RBS spectra recorded for Au contacts deposited by different methods (thermal evaporation, sputtering and electroless).

¹ CGL, Physics Department, Autónoma University of Madrid, Spain.

Formation of transition metal nitrides by N⁺ ion implantation

A.R.G. Costa², M.M. Cruz^{1,2}, M. Godinho^{1,2}, N. Franco, R.C. da Silva

Seeking for magnetic metal nitrides, iron, cobalt and nickel plates of purity 99.9% were implanted at room temperature with 50 keV N⁺ ions to fluences of 2×10^{17} cm⁻² and 5×10^{17} cm⁻², in order to study the influence of implanted nitrogen concentration in the production of nitride phases. Rutherford Backscattering Spectrometry with 2 MeV He⁺ ions along with the RUMP code allowed calculating the effective implanted fluences as $\sim 1.9 \times 10^{17}$ cm⁻² and $\sim 3.5 \times 10^{17}$ cm⁻² respectively. The presence of nitride phases Fe₂N and Ni₃N was detected by XRD. Conversion Electron Mossbauer Spectrometry was also used with the iron samples, showing the presence of Fe₂N and also different Fe₃₋₈N phases after annealing at 250 °C. Iron and cobalt single crystals with different orientations were implanted at room temperature with 5×10^{17} cm⁻², 50 keV N⁺ ions⁺, under 10° incidence angles to avoid channelling effects. The effective fluence was evaluated as $\sim 3.4 \times 10^{17}$ cm⁻² for cobalt and (110) Fe crystals, and $\sim 3.0 \times 10^{17}$ cm⁻² for the (100) and (111) Fe crystals. Phase identification in both cobalt and iron crystals by XRD showed that Co₂N forms in *m*-cobalt but not in *c*-cobalt, while Fe₂N was identified for all Fe crystal orientations.

¹ Dep. Física, FCUL; ²CFMC, UL.

Characterization of neutron irradiated Be samples

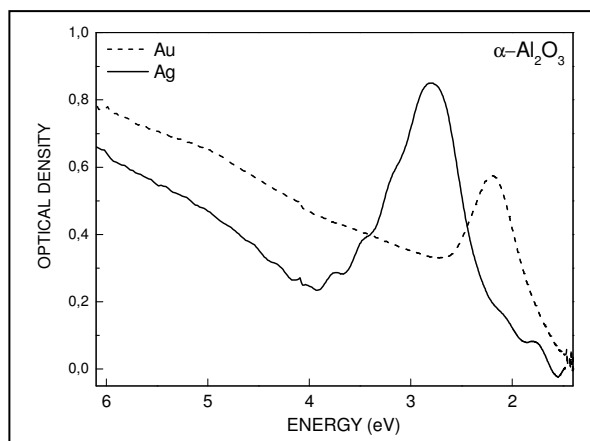
L.C. Alves, E. Alves, N. Catarino

Related with the study of advanced fusion reactor materials, four sets of Be pebbles and two different composition Ti beryllide samples, all of them subjected to a high neutron flux irradiation, were analysed with Ion Beam Analytical techniques using a Nuclear Microprobe. The main objectives were to determine possible structural changes after irradiation and extent of surface oxidation. Complementarily, gamma spectra were accumulated once the samples presented a low level of induced radiation. Comparison on the oxidation behaviour of the sets of pebbles provided by the same manufacturer but with different diameter size (0.5 mm and 1 mm) was also established as well as the dependence with irradiation temperature (425 °C, 525 °C and 750 °C). Surface oxidation extent showed no relevant dependence on pebble size although within one of the sets the ‘typical’ behaviour was difficult to established, with some of the pebbles presenting heavy N contamination of unknown origin.

Surface morphology, thermal and electrical conductivity of α -Al₂O₃ single crystals implanted with Au and Ag ions

B. Savoini¹, M. Tardío¹, R. Ramírez¹, C. Marque, E. Alves

α -Al₂O₃ single crystals with *c*, *m* and *r* orientations, ion implantation at room temperature, with Au or Ag ions, energy of 160 keV and fluences ranging from 5×10^{15} to 1×10^{17} ions/cm². The presence of metal precipitates was explored by AFM and monitored by the variation of the intensity of the extinction bands associated with Mie scattering from Au and Ag colloids located at about 2.2 eV (563 nm) and 2.8 eV (443 nm), respectively (Fig.). The results show a dependence on the surface roughness with the ion fluence and the implantation orientation. The *I-V* characteristic of the electrical contacts reveals an ohmic behaviour, independent of the ions implanted and the crystallographic orientation. Measurements of the electrical conductivity at different temperatures in the investigated range predominantly suggest a band conduction mechanism thermally activated, with energies of about 0.09 eV and 0.07 eV, in samples implanted with Au or Ag ions, respectively. We conclude that the enhancement in conductivity observed in the implanted regions is related to the intrinsic defects created by the implantation, rather than to the implanted Au and Ag ions.



¹Universidad Carlos III de Madrid, Leganés (Madrid), Spain.

TiN_x coated polycarbonate for bio-electrode applications

P. Pedrosa^{1,2,4,5}, E. Alves, N.P. Barradas, P. Fiedler³, J. Hauelsen³, F. Vaz⁴, C. Fonseca^{1,2,5}

Titanium nitride (TiN_x) thin films were deposited by PVD, in a wide range of compositions ($0 < x < 0.99$), on polycarbonate (PC) substrates, aiming at studying their potential application as bio-electrodes. The electrochemical study of the TiN_x films, performed in an isotonic sodium chloride solution, proved the very good chemical stability of all films in salt solution conditions. On the other hand, the electrochemical noise analysis showed that the electrical noise generated at the stoichiometric TiN/electrolyte interface is of the same magnitude as that generated by the traditional Ag/AgCl electrodes. The lower impedance values of the films will facilitate bio-signal transfer in the presence of a sweat layer.

¹ Departamento de Engenharia Metalúrgica e de Materiais, Universidade do Porto, Portugal.

² SEG-CEMUC – Universidade de Coimbra, Portugal.

³ Institute of Biomedical Engineering and Informatics, Ilmenau University of Technology, Germany.

⁴ Centro de Física, Universidade do Minho, 4710-057 Braga, Portugal.

⁵ INEB – Instituto de Engenharia Biomédica, Divisão de Biomateriais, Universidade do Porto.

The width of an RBS spectrum revisited: influence of multiple scattering

N.P. Barradas

P. Bauer, E. Steinbauer, and J.P. Biersack calculated with Monte Carlo the RBS spectrum of 100 keV protons backscattered from a 100 nm thick Au foil (P. Bauer et al. NIM B64 (1992) 711). They stated in the caption of Figure 2 that a fairly large area, located to the left of the single scattering signal, “corresponds to the contribution due to multiple scattering”. This led to the widespread belief amongst code developers that “multiple scattering manifests itself mostly as an additional contribution to the energy spread and as small low energy tails on signal edges arising from non-Gaussian wings in the energy distribution. (...) The small tails have not, so far, been modelled analytically.” (E. Rauhala et al. NIM B244 (2006) 436. A new analytical calculation is now presented, showing that an extra yield due to multiple scattering indeed exists, but it is much smaller than the hatched area in Figure 2 of Bauer et al. That area is not an additional contribution of multiple scattering, it is simply the width of the low energy edge of the single scattering signal, which is broader due to the extra energy spread coming from multiple scattering.

The electronic transport mechanism in indium molybdenum oxide thin films RF sputtered at room temperature

E. Elamurugu¹, P. Shanmugam¹, G. Gonçalves¹, R. Martins,¹ E. Fortunato¹, N. Franco, E. Alves

Indium molybdenum oxide (IMO) thin films were radio-frequency (RF) sputtered at room temperature (RT) and studied as a function of base pressure (BP). The crystallinity of the films is decreased with the increase in BP. A maximum mobility (μ) of $49.6 \text{ cm}^2 \text{ V}^{-1} \text{ s}^{-1}$ was obtained from the IMO films deposited at RT without any post-annealing treatment. The electronic behaviour of the deposited films was investigated by temperature dependent (100-550K) Hall measurements. Study on the scattering mechanisms based on the experimental data and theoretical models show that the ionized scattering centres are dominating. The films possess wide work function (4.91 eV) and high transmittance (> 70 %) over visible-near infrared (NIR) range. The results obtained, especially the high work function and NIR transmittance, are promising that the deposited IMO films may be useful in the applications such as solar cells.

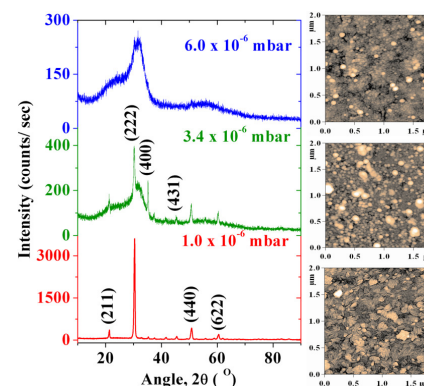


Fig. 1- XRD patterns of IMO films as a function of base pressure; AFM microstructures are shown next to the corresponding XRD

¹ CENIMAT/I3, FCT, Universidade Nova de Lisboa, Portugal.

Structural characterization of FeSiBCuP samples melt quenched under high gravity

R.M.S. Martins, I. Takeuchi¹, Y. Furuya², N. Schell³

Considerable attention is devoted to Fe-based magnetic nanocrystalline alloys, which show excellent soft magnetic properties. However, an efficient control of their average grain size is required for a significant decrease of the effective magnetic anisotropy. At Hirosaki University in Japan, FeSiBCuP nanocrystalline soft magnetic alloys were prepared by ultra high G quenching technique. Here, we report the experiments carried out at the High Energy Materials Science beam line HEMS at PETRA III, DESY, which offers excellent research possibilities to investigate fine structural details. The α -Fe phase was found to be the primary phase present in the studied samples. Fe₂B was also noticeably in all samples. X-ray diffraction patterns obtained for samples with Fe 83.3 at% and with Fe 85.3 at%, processed under the same gravity conditions (5000 G), showed that the formation of Fe₃B compounds is much more pronounced for the sample with higher Fe content. The study of samples with Fe 87.3 at% processed under 4000 G and 5000 G showed that higher gravity conditions promote the development of Fe₃B compounds.

¹ University of Maryland, USA, ² Hirosaki University, Japan, ³ Helmholtz-Zentrum Geesthacht, Germany.

Study of new colouration processes in glasses

M. Ventura^{1,2}, A. Ruivo^{2,3}, A.P. Matos², L.C. Alves, R.C. da Silva

As part of a collaboration research on new processes of colouring glasses, industrial float glasses were colour doped with noble metal ions of Cu, Ag, and/or Au. The coloured glasses had both their faces characterized by RBS and PIXE, seeking at understanding the role of Sn in the final depth distribution and aggregation state of the noble metal ions in the glass matrix, in correlation with the observed colours. The results obtained so far show that in the case of Cu-doping by spray pyrolysis onto hot glass surfaces, Cu concentrates at the surface reaching to higher concentrations in the Sn-bearing faces, diffusing inwards and developing only a red tint upon annealing. In contrast, the glasses doped by dipping in mixtures of molten Cu compounds display a strong ruby red colour and correspondingly intense SPR optical band, along with much stronger Cu $K\alpha$ intensities in their XRF spectra, but significantly lower RBS yields that extend to low energies. This is a clear indication of extensive diffusion with formation of a large number of Cu nanoparticles, evenly dispersed along several micrometres from the surface of the glass matrix. As the effect is much more marked in the Sn-bearing face Sn does have a role in the colouring process. In the cases of Ag and Au colouring by thermal reduction of a multi-layered polyelectrolyte dip coatings doped with the noble metal ions, the RBS and PIXE analysis indicate generically similar trends: Ag and Au tend to concentrate more in the Sn-bearing faces.

¹ DCR/FCT-UNL; ² VICARTE/FCT-UNL; ³ REQUINTE/FCT-UNL.

Limited angle STIM-tomography

A.C. Marques, D. Beasley, L.C. Alves, R.C. da Silva

Building on work initiated in 2010, preparing the setup and software for ion beam tomography, morphological characterization of SiC grains (~30 μm in diameter) immobilized in formvar fibers was performed by STIM tomography in off-axis geometry. The data gathered allowed morphological reconstruction and showed it will allow determining 3D density distribution. Despite the improvements made on the existing setup and procedures, there remain positioning and alignment problems with the rotation axis: some degree of misalignment seems inevitable. Two types of solution were devised to mitigate these problems: *i*) assembly of a positioning stage with 5+1 degrees of freedom is being implemented, and *ii*) pre-processing software with alignment algorithm was developed and tested. Aiming at better reconstruction an algorithm allowing the efficient removal of background noise was also implemented. These were integrated in a common graphical user interface, *TomoAlign*. Use of the BFP-based *Tomo3D* software shows that a reasonable reconstruction is achievable after suitable data pre-processing of digital alignment (cf. Fig.1).

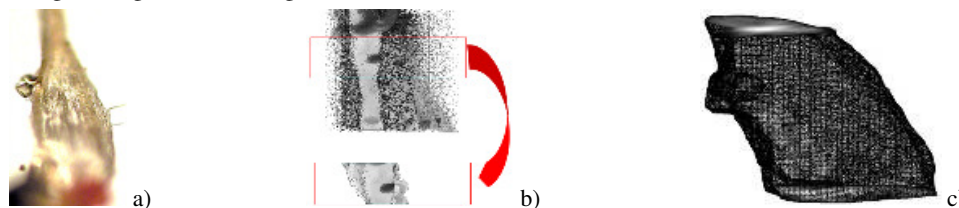


Fig.1 a) Microscope image of the STIM-T analyzed formvar fiber with SiC grains; b) projections acquired over 180° rotation range in steps of 10° (top), and one section cropped after pre-processing (bottom). By BFP the 3D image in (c) was obtained. Besides alignment corrections pre-processing included the removal of noise and of spikes.

Synchrotron radiation-based micro-computed tomography applied to study embryonic dinosaur fossils

R.M.S. Martins, F. Beckmann², R. Castanhinha^{1,3}, O. Mateus^{1,4}, R. Araújo^{1,5}, P.K. Pranzas²

One of the most relevant specimens of the Museum of Lourinhã is the nest found in Paimogo, in 1993, with embryos attributed to the theropod dinosaur *Lourinhanosaurus antunesi*. In this nest more than 100 eggs or eggshell concentrations were detected. The embryonic remains were found as isolated skeletal elements in ovo or in close association with eggs. The site is late Jurassic in age, which fills an important temporal and phylogenetic gap of the fossil record regarding theropod embryos. Furthermore, it belongs to a clade widely regarded as ancestors of birds. Several embryonic vertebrae have been studied by Synchrotron Radiation-based Micro-Computed Tomography (SRμCT) at the BW2 beam line. We have obtained high-resolution 3D tomographic datasets using a non-destructive procedure. A photograph showing a dinosaur embryonic vertebra (ML565_Paim55) found in the Paimogo nest is presented in Fig. 1 (a). The specimen was imaged by microtomography in absorption mode with photon energy of 24 keV. Microtomographic slices through the vertebra are shown in Fig. 1 (b)-(c). The exquisite anatomical and histological preservation of the embryonic bones will allow observations of unprecedented precision and detail for theropods. This material allows us to extend in time and to considerably supplement in great detail our knowledge of early ontogeny of carnivorous dinosaurs.

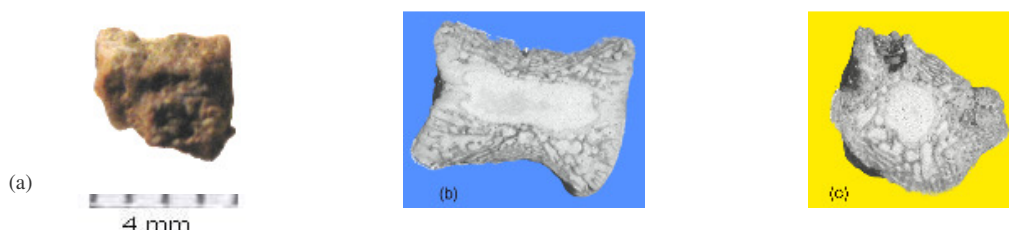


Fig. 1- Embryonic vertebra of *Lourinhanosaurus antunesi* found in the nest recovered from Paimogo site: (a) photograph of the vertebra; (b) longitudinal section of the vertebra; (c) general view of a centrum cross-section of the vertebra.

¹ Museu da Lourinhã, Portugal; ² Helmholtz-Zentrum Geesthacht (HZG), Germany; ³ IGC, Portugal; ⁴ FCT, Universidade Nova de Lisboa, Portugal; ⁵ HDES, Southern Methodist University, USA.

Hydrogen retention in W-Ta composites proposed for use in first wall applications

R. Mateus¹, M. Dias, J. Lopes², J. Rocha, V. Livramento^{1,3}, J.B. Correia^{1,3}, P.A. Carvalho^{1,4}, K. Hanada⁵, E. Alves

In opposition to W-Ta alloys, in W-Ta composites the individual phases remain quite separated within the microstructure and the behaviour of the final material under irradiation depend of the properties of pure components. W and Ta plates and W-Ta composites consolidated via spark plasma sintering (SPS) were implanted with energetic He⁺ and D⁺ ion beams at different temperatures (RT, 200 and 400 °C). The pre implantation with He⁺ induces the blistering of the He enriched surfaces, in particular in the Ta phase. However, the induced retention of D is only significantly increased in W plates while for Ta the increment is much weaker. This behaviour is explained by the lower radiation resistance of W relatively to Ta. As a consequence, hydrogen retention in W-Ta composites is preferentially associated to the W component and to the composite production route. The results also evidence that the hydride phase (Ta₂H) in pure Ta is not stable at higher temperatures. Furthermore, the hydride phase could be avoided in the W-Ta composites by controlling the SPS consolidation temperature and the interdiffusion between the components, which is moderate below 1300 °C due to mainly diffusion of W into Ta.

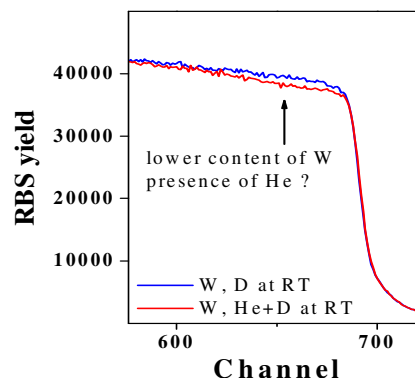


Fig. 1- RBS spectra of pure W implanted with ²H and ²H+⁴He.

¹ Instituto de Plasmas e Fusão Nuclear, Instituto Superior Técnico, Lisboa, Portugal; ² Instituto Superior de Engenharia de Lisboa, Lisboa, Portugal;

³ Laboratório Nacional de Energia e Geologia, Lisboa, Portugal;

⁴ ICEMS, Departamento de Bioengenharia, Instituto Superior Técnico, Lisboa, Portugal;

⁵ AIST, National Institute of Advanced Industrial Science and Technology, Tsukuba, Japan.

Determination of stopping powers of different ions in different systems

N.P. Barradas, E. Alves, Z. Siketić¹, I.B. Radović¹

The knowledge and amount of stopping power measurements available for heavy ions is much smaller than for H and He, with negative consequences for the accuracy of calculational schemes such as SRIM. We used a bulk method, previously developed by us and applied successfully to other systems, to determine experimentally the stopping power of He, C and O in Si, GaN and TiO₂. This is particularly useful for heavy ion elastic recoil detection analysis, given that Si is one of the most commonly analysed materials, and C and O are light elements which quantitative determination is ideally made by HI-ERDA. We compare the results with SRIM and MSTAR as well as with other data.

¹ Ruđer Bošković Institute, P.O. Box 180, 10002 Zagreb, Croatia.

Improving the CASSIS code for channelling computer simulations

A. Kling

Ion channelling is very powerful for the study of the real structure of monocrystalline materials (e.g. lattice site of foreign atoms, intrinsic defects, etc.). The development of the CASSIS code started more than a decade ago and continuously yielded extensions to investigate additional channelling phenomena (e.g. the influence of the incident angle on the channelling spectra in catastrophic dechannelling at strained layers interfaces, simulation of extended 3D-defects etc.). Due to the enormous progress in computer technology it was necessary to refurbish parts of the existing code by updating calculation methods using more detailed and/or higher precision algorithms. A long-standing problem was the lack of user-friendliness of the code. This has been resolved by introducing a simple input procedure for the most common channelling problems that is assisted by several automatic procedures (e.g. determination of the crystallographic system and the necessary vectors for the simulation from the input data). The improved speed of the program allows now also the calculation large-dimension 2D-scan plots that may be useful for the determination of useful crystallographic directions in complex crystalline systems not studied so far.

Laboratory operation and development – accelerators data acquisition and motion control automation

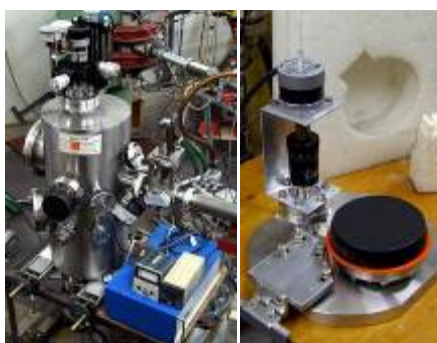
N. Catarino, C. Cruz, E. Alves, L.C. Alves, R.C. da Silva

Previously detected functional instabilities in the interplay with the data acquisition software lead to a thorough revision of the goniometers motors automation control code. The causes were identified and the problem solved by changing the execution of critical external calls to synchronous mode operation. This further allowed elimination of delay patches making the code faster. The code sections related to the interaction with the data acquisition software, protections of mutually exclusive operations, and with the switching of control between experimental setups, were also rewritten in optimized form adding to its operational robustness. As part of code revision three important new features were introduced: *i)* an instance was added allowing automatic acquisition of long series of IBA spectra in repetitive characterization experiments of JET related materials; *ii)* an instance was developed allowing the execution of random spectra in RBS/C experiments, by sampling over user defined sets of coordinates, and *iii)* the simple graphical display of angular scan data was enhanced with new functionalities, among which: split/merge of individual scan data sets, vertical and horizontal scale expansion/compression, and selection of sub-scan and call to the viewing window.

Installation, test and implementation of the JET chamber and a new IBA beam line

N. Catarino, C. Cruz, L.C. Alves, R.C. da Silva, E. Alves

An experimental chamber dedicated for IBA characterization of JET related materials was received from Sussex University and installed as a removable insert in the PIXE beam line. For this a support base and sliding system were designed and manufactured enabling the alignment of the chamber and its removal when not in use. After successfully testing operational status was achieved by collecting RBS and NRA spectra, under correct measurement of the beam charge, a new stepping motor was fitted to the target loading port to allow automatic acquisition of IBA spectra during repetitive characterization experiments, under remote computer control.



In order to make operational a new multipurpose IBA beam line on the 3 MV tandem accelerator facility, endowing it with RBS/NRA/PIXE in combination with channelling, a new electronic drive system was planned for control and of the goniometer stepping motors and automation of the experiments. Contrary to the proprietary systems developed in-house two decades ago, and still in operation in the 2.5 MV VG accelerator facility, an off-the-shelf commercial solution was chosen, based on two RS 217-3611 stepper motors activation boards and one RS 440-098 programmable control board with built-in control firmware. These Eurocard boards intercommunicate via a 2x32 way-to-1x64 way DIN 41612 connectors and allow computer control through standard RS-232C ports. A control program was developed for testing the new system and preparing its integration in existing automation code.

Installation and optimization of a rapid thermal annealing furnace

S.M.C. Miranda, N. Catarino, E. Alves, K. Lorenz

Rapid thermal annealing (RTA) equipment (“AS-one 100” by Annealsys) was installed and tested for sample processing up to 1500 °C. It is capable of reaching temperatures up to 1500 °C in vacuum or gas atmospheric pressure using fast heating and cooling ramps. On-site facilities (power- and water supply) were installed in order to operate the RTA furnace. A gas supply system was projected and assembled which allows for annealing in N₂, Ar, and NH₃/N₂ atmospheres. RTA process operation and annealing recipes were optimized in order to improve functionality and safe handling, obtain reproducible results, and reduce overshooting above the desired anneal temperature. Annealing procedures and parameters were optimized for implant activation in GaN thin films. The adequate heat ramp setting was found to be 30 °C/s and the highest temperature that could be reached without inducing dissociation of the sample was 1200 °C in NH₃ containing atmosphere. NH₃ was found to stabilize the surface and reduce the out-diffusion of nitrogen.

Laboratory operation and development

A.R.G. Costa^{1,2}, R.C. da Silva

A prototype of an acid saw was designed, developed and assembled for cutting metal crystals producing the least damage by mechanical deformation. The cutting action is achieved by an acid soaked fiber wire undergoing a reciprocating movement with a net positive displacement, using two stepping motors (NMB PM55-048), which are controlled by an open-source single-board microcontroller Arduino®, via a driving circuit designed in-house that supplies the necessary power, under control of the microcontroller based firmware. The controlling code was developed in a proprietary ANSI-based C language and uploaded into the microcontroller.

¹ Dep. Física, FCUL; ² CFMC, UL.